Scientific Research Publishing

Open Journal of Applied Sciences, 2025, 15(11), 3462-3477
https://www.scirp.org/journal/ojapps
ISSN Online: 2165-3925
ISSN Print: 2165-3917

Evaluation of the Behavior of a 3 MW Wind Warm with a Permanent Magnet Synchronous Generator under the Wind Conditions of Benin

Assane Ogoubiyi[1], Richard Gilles Agbokpanzo[1], Arouna Oloulade[2]

[1]LARPET, University of Abomey (UNSTIM), Abomey, Benin
[2]LETIA/EPAC-UAC, University of Abomey-Calavi, Abomey-Calavi, Benin
Email: Ogoubiyiassane2@gmail.com, richgille@gmail.com, olouarou@yahoo.fr

How to cite this paper: Ogoubiyi, A., Agbokpanzo, R.G. and Oloulade, A. (2025) Evaluation of the Behavior of a 3 MW Wind Warm with a Permanent Magnet Synchronous Generator under the Wind Conditions of Benin. *Open Journal of Applied Sciences*, **15**, 3462-3477.
https://doi.org/10.4236/ojapps.2025.1511223

Received: October 21, 2025
Accepted: November 2, 2025
Published: November 5, 2025

Abstract

Faced with Benin's electricity deficit and dependence, which cause imbalances in its power system, the exploitation of wind energy has become a necessity. The ability of wind turbines to contribute to the stability of transmission networks improves significantly when high-power units are used. However, this capability is complicated by the intermittent and random nature of wind. For optimal operation, a robust wind turbine system must be able to extract maximum power under low wind speeds and limit it under high wind conditions through its control system. The E115/3MW wind turbine generators are multipole ring-type synchronous machines with very high efficiency. Moreover, the trend is moving toward permanent magnet synchronous generators (PMSG), which offer better efficiency but are exposed to the risk of demagnetization. Within the limits of magnetic saturation, our study aims to evaluate the performance of an E115/3 MW wind turbine equipped with a Permanent Magnet Synchronous Generator (PMSG) under the wind conditions of Benin. The torque control strategy without speed feedback used in this study enabled us to extract the maximum power from the wind. The pitch angle control, based on a simple electric actuator, effectively limited the output power to 3 MW, demonstrating the system's robustness. For wind speeds around 11.5 m/s, the turbine delivered power levels close to 3 MW, proving suitable for the Sèkandji site. Finally, vector control of the stator currents improved the overall performance of the PMSG.

Keywords

Modeling, Wind Farm, Control, Permanent Magnet Synchronous Generator, Pitch Angle

1. Introduction

From 2000 to 2020, the global wind energy market grew from 17.4 GW to 743 GW, with an average annual growth rate of about 12.6%, driven by the development of variable-speed technologies. With the increasing demand for electricity, projections indicate that wind energy will reach 29.1% in 2030 and 34.2% in 2050 [1] [2]. Benin, characterized by an electricity deficit and dependence on increasingly scarce fossil energy sources, often faces instability issues within its power grid. To address this energy challenge, Benin relies on its photovoltaic potential and aligns its energy policy with the renewable energy production projects promoted by ECOWAS for the 2019-2033 period. To maintain the balance between supply and demand, the construction and connection of new production units using inertial renewable sources such as wind turbines should be considered. Increasing production capacity contributes to the stability of the transmission network. However, the integration of wind energy into the national energy mix remains conditional upon favorable wind conditions and the advancement of wind power technologies [3]-[5].

Variable-speed wind turbines offer the ability to capture the maximum possible energy from wind, which is inherently random and intermittent [6]. They have accelerated the development of large-scale wind turbine systems capable of contributing to the stability of transmission networks, thus justifying their use in large industrial applications. These systems are based on asynchronous and synchronous machines. Unlike wind turbines using asynchronous generators, those based on synchronous generators with a high number of pole pairs and permanent magnets (PMSG) operating at low speed do not require slip rings, brushes, or gearboxes. This significantly reduces maintenance costs, especially for offshore wind projects [7] [8]. Wind turbines operate in four distinct zones, but mainly in two: the partial-load zone for low wind speeds and the full-load zone for medium and high wind speeds.

To extract the maximum power during partial-load operation, wind turbines use Maximum Power Point Tracking (MPPT) techniques, which are divided into two categories. The speed-sensorless MPPT technique, based on wind speed estimation, allows indirect adjustment of the turbine's mechanical rotational speed to its optimal value, enabling maximum power extraction for any wind speed below V_{WN} [9] [10]. However, this estimation-based strategy depends on the specific characteristics of the wind turbine, even though it remains simple, fast, independent of direct wind measurement, robust, and easy to implement [11]. It is widely used in direct-drive wind turbines to facilitate the development of vector control strategies for electrical quantities such as current or power [12] [13].

In contrast, during full-load operation, due to the mechanical load constraints of the turbine and the operating limits of the power converter in a PMSG designed for 100% of the rated power, the wind turbine system must be protected by a power-limitation mechanism [14]. Effective pitch angle control enables this limitation even under highly turbulent and strong wind conditions. A first-order control system is sufficient to achieve proper regulation of the blade pitch orientation.

Furthermore, any control strategy for the PMSG must contribute to improving

its performance and, consequently, the overall performance of the entire system [15] [16]. Moreover, the E-115 3 MW variable-speed wind turbines supplied by ENERCON, featuring direct-drive systems and active pitch control, are of great interest for wind sites due to their high-power coefficient [17] [18].

In the context of harnessing Benin's wind potential, the question arises of how to ensure the optimal operation of a 3 MW wind turbine under fluctuating wind conditions at a Beninese site and which wind technology is most suitable. The objective of this study is to evaluate the behavior of a 3 MW wind turbine with a Permanent Magnet Synchronous Generator (PMSG) under the wind conditions of Benin. To achieve this objective, we formulated two hypotheses. Modeling the wind turbine system allows for the evaluation of its behavior under variable wind conditions. The implemented control laws improve the overall performance of the wind turbine system.

2. Materials and Methods

2.1. Presentation of Research Diagram

Figure 1 presents the research diagram of the study. The process begins with the characterization of the E-115/3 MW wind turbine and the wind profile at a site in Benin. Subsequently, the wind profile, the wind turbine, and its shaft are modeled, along with the PMSG. Based on these models, a simple MPPT control strategy is developed, followed by the pitch angle regulation algorithm and the vector control of the PMSG. The capability of the wind turbine system and its control to deliver power under low, medium, and high wind conditions is then evaluated. The robustness of this controller will be assessed under realistic and strong wind conditions at a wind site in Benin.

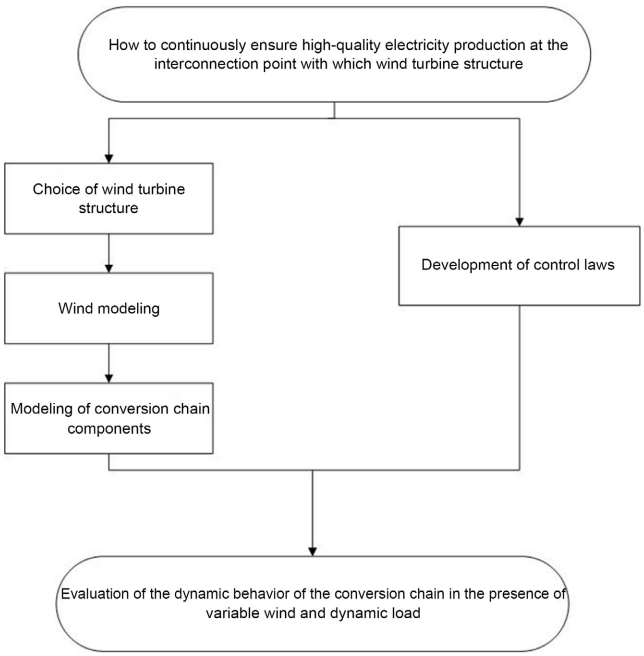

Figure 1. Research diagram.

2.2. Presentation of the Wind Turbine Characteristics and Wind Profile Data

- Technical Data of the E-115/3 MW Wind Turbine

Direct-drive technologies (without gearboxes) have the advantage of contributing to grid stability while reducing mechanical wear on components [16]. The EP5-type E115-3 MW direct-drive wind turbines with ring-type permanent magnet synchronous generators are an improved version of the EP3 turbines, which are directly coupled to a multipolar synchronous generator with separate excitation. The technical data of the E115-3 MW turbine are presented in **Table 1**.

- Characteristics of the wind Profile at 100 m Above Ground

Due to its proximity (38 km) to the 161 kV WAPP network in Sakété, an interconnection point, and its wind profile suitable for variable-speed wind turbines, the Sèkandji site has been selected for the study. **Table 2** provides the parameters used for the wind speed simulation.

After modeling the turbine and the control laws, the technical data of the wind turbine and the wind profile will be used for simulation and validation of the results using Matlab/Simulink software.

Table 1. Technical data of the E-115/3 MW [17].

	Technical Data of the Wind Turbine	
	Characteristics	Values
Characteristics of the 115 m/3 MW wind turbine	Nominal Power	3000 kW
	Starting speed	2 m/s
	Nominal Wind speed	11.5 m/s
	Wind speed at disconnection	25 m/s
	Rotor blade diameter	115.7 m
	Swept area of the roto	10515.5 m^2
	Number of blades	3
	Rotational speed, max:	12.8 U/min
	Tip speed	78 m/s
	Hub height	92 m
	Rotor rotational speed	4 - 12.4 tours/min
	Reference pitch angle	1˚

Table 2. Simulation parameters for the realistic wind speed at the Sèkandji site.

		Characteristic data of the wind profile		
		Parameters	Value	Unit
Parameters of the realistic wind model	Wind characteristics	Average wind speed	7.9544	m/s
		Scaling factor	9.4669	m/s
		Shape factor	1.9065	
		Average of variations	0.1	m/s
	Data of the filter and the number-generating function	Filter time constant T_w	0.5	s
		Sampling period	0.1	s

2.3. Wind Modeling

A realistic wind at a given site is composed of two components: the mean wind V_{vm} and the fluctuating component v_v, which represents variations caused by turbulent winds. Its profile is generated using Equation (2) [19].

$$v_v(t) = \left(\frac{-\ln(\text{rand}(t))}{C_w} \right)^{\frac{1}{K_w}} \tag{1}$$

$$V_v(t) = \left(1 + v_v(t) - V_{vvm}\right) V_{vm} \tag{2}$$

where v_v is the magnitude of the function rand(t), which generates a sequence of random numbers between 0 and 1 following a uniform distribution and conforming to the Weibull distribution. K_w is the shape factor and C_w is the scale factor calculated from the Weibull breakdown at hub height. V_{vvm} represents the average wind variations at the site.

The very high-frequency components can be removed from the wind profile by filtering the wind speed generating function using Equation (3), which allows taking into account the mean velocity gradient across the entire surface of the turbine rotor [19].

$$H_{V_v} = \frac{1}{1 + sT_{vv}} \tag{3}$$

2.4. Modeling of the Wind Turbine Dynamics

The modeling of the wind turbine system concerns the wind motion, the aerodynamic conversion of the turbine, and the shaft dynamics.

- Aerodynamic conversion of the turbine

The wind turbine captures a portion of the power contained as kinetic energy in the wind passing through the area swept by the turbine. Betz's theory, which allows the evaluation of the aerodynamic power P_{tu} delivered by the wind turbine, is represented by Equation (4).

$$P_{tu} = \frac{1}{2} C_p(\lambda, \beta) \cdot \rho_V \cdot S_p \cdot V_v^3 \tag{4}$$

where

- V_v is the upstream wind speed (m/s).
- C_p is the power coefficient of the wind turbine (theoretical maximum value 0.593) [20].
- ρ_V is the air density (1.225 kg·m^{-3}).
- S_p is the area swept by the rotor blades (m^2) with radius R_{pt} (m).

The tip speed ratio, denoted by λ, characterizes the ratio between the blade peripheral speed U and the wind speed V_v [20] and is given by Equation (5).

$$\lambda = \frac{U}{V_v} = \frac{\Omega_{tu} R_{pt}}{V_v} \tag{5}$$

With Ω_{tu} being the angular rotation speed of the blades in rd/s.

The aerodynamic efficiency C_p as a function of the pitch angle β and the tip speed ratio λ is generally defined by empirical formulas. However, there are formulas implemented in MATLAB for large three-bladed turbines developed in [21] and [22], presented in Equation (6) and Equation (7).

$$c_p = C_1\left(\frac{116}{\lambda_i} - 0.4\beta - 5\right)\mathrm{e}^{\frac{-21}{\lambda_i}} + 0.0068\lambda \tag{6}$$

$$\lambda_i = \left(\frac{1}{\lambda + 0.08\beta} - \frac{0.035}{\beta^3 + 1}\right)^{-1} \tag{7}$$

C_1 is a coefficient used to adjust C_p for the aerodynamic power at the rated point provided by the manufacturer.

The wind torque T_{tu} developed by a wind turbine rotating at the angular speed Ω_{tu} is described by Equation (8) and Equation (9)

$$T_{tu} = \frac{P_{tu}}{\Omega_{tu}} \tag{8}$$

$$T_{tu} = \frac{1}{2}\frac{C_p(\lambda,\beta)\cdot\rho_V\cdot S_p\cdot V_v^3}{\Omega_{tu}} \tag{9}$$

- Shaft Dynamics model

The generator shaft, mechanically linked to the rotor blades, converts mechanical energy into electrical energy. The mechanical torque seen by the directly coupled synchronous machine is different from that developed by the turbine. Indeed, the intrinsic viscous friction and the inertia of the wind turbine generate dynamics that oppose the turbine structure. This can be expressed mathematically by Equation (10).

$$J_{tg}\frac{\mathrm{d}\Omega_{mec}}{\mathrm{d}t} + f_v\cdot\Omega_{mec} = T_{tu} - T_{emg} \tag{10}$$

With

T_{emg} : Electromagnetic torque produced by the generator.

f_v : Viscous friction coefficient.

Ω_{mec} : Mechanical rotational speed of the generator.

J_{tg} : Turbine moment of inertia (kg·m^2).

- PMSG Modeling

The machine is modeled in the Park reference frame. Assuming that the rotor flux vector coincides with the "d" axis of the synchronous (d,q) frame and neglecting the homopolar component [16], the expressions for the output current vector components are given by Equation (11), and the electromagnetic torque by Equation (12)

$$\begin{cases} \dfrac{\mathrm{d}i_{gd}}{\mathrm{d}t} = \dfrac{i}{L_d}\left(-V_{gd} - R_{gss}i_{gd} - \omega_g L_q\cdot i_{gq}\right) \\ \dfrac{\mathrm{d}i_{gq}}{\mathrm{d}t} = \dfrac{i}{L_q}\left(-V_{gq} - R_{gss}i_{gq} - L_q + \omega_g\left(L_q\cdot i_{gd} - \Psi_{sm}\right)\right) \end{cases} \tag{11}$$

o Electromagnetic Torque Equation

$$T_{emg} = \frac{3}{2} p\left(i_{gq} \cdot \Psi_{sm} - \left(L_d - L_q\right) i_{gd} \cdot i_{gq}\right) \tag{12}$$

o The inductances of the coils along the d and q axes

Synchronous machines with a large number of poles have smooth poles, and the assumption given by relation (13).

$$\begin{cases} L_d = L_S \\ L_q = L_S \end{cases} \tag{13}$$

Thus, the expression of the electromagnetic torque becomes (14)

$$T_{emg} = \frac{3}{2} N_p \left(i_{gq} \cdot \Psi_{sm}\right) \tag{14}$$

where N_p is the number of pole pairs of the synchronous generator.

The angular frequency of the sinusoidal quantities is defined by (15)

$$\omega_g = N_p \cdot \Omega_{meca} \tag{15}$$

2.5. Development of Control Lows

The control laws concern the strategies for controlling the dynamics of the wind turbine and the electrical conversion system to optimally exploit the potential of the wind site.

- MPPT without feedback control

The MPPT technique without speed control based on wind speed estimation allows indirect adjustment of the mechanical rotation speed of the turbine to its optimal value, as indicated by the expression (16)

$$T_{em\_ref} = K_{op} \cdot \Omega_{mec}^2 \tag{16}$$

where

$$K_{op} = \frac{C_{p\max}}{\lambda_{opt}} \frac{\pi \cdot R_{pt}^5 \rho_V}{2} \tag{17}$$

- Modeling of the pitch controller

The proposed pitch controller is based on a proportional controller that amplifies the rotational speed error over a wide wind speed range from 1 m/s to 25 m/s. A memory placed after the controller allows the regulator to track the wind dynamics and adjust the pitch angle to optimize and limit the power to its rated value. Its algorithm is provided by the block diagram in **Figure 2**.

- Vector control of the PMSG

In vector control, the stator flux is oriented so as to independently control the electromagnetic torque, similar to a DC machine, by decoupling the (dq) components of the stator current [23]. The commonly used control consists of setting the direct-axis current to zero [24]. Thus, with the stator-induced flux Ψ_{sm} kept constant, the q-axis current provides the reference value of the electromagnetic torque according to Equation (18) [24]-[28].

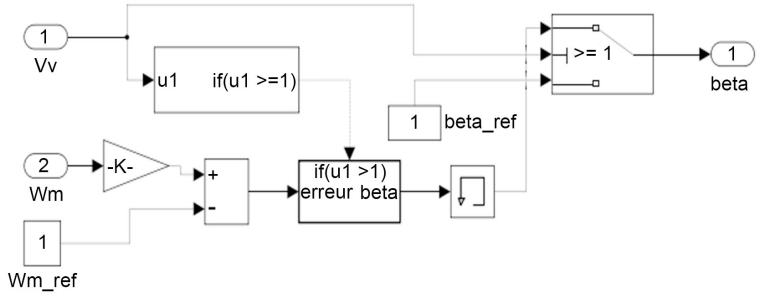

Figure 2. Block diagram of the pitch controller.

$$T_{emg\_ref} = \frac{3}{2} N_p \left(\Psi_{sm}\right) i_{gq\_ref} \tag{18}$$

The reference quadrature current is given by Equation (19).

$$i_{gq\_ref} = \frac{2}{3N_p \Psi_{sm}} T_{emg\_ref} \tag{19}$$

The control voltages V_{gd} and V_{gq} are generated by compensating the (dq) coupling components of the voltages according to Equations (20) and (21).

$$\begin{cases} V_{gd\_ref} = -R_{gss} i_{gd} - L_d \cdot \dfrac{\mathrm{d}i_{gd}}{\mathrm{d}t} \\ V_{gq\_ref} = -R_{gss} i_{gq} - L_q \cdot \dfrac{\mathrm{d}i_{gq}}{\mathrm{d}t} \end{cases} \tag{20}$$

$$\begin{cases} V_{gd} = V_{gd\_ref} - \omega_g L_q \cdot i_{gq} \\ V_{gq} = V_{gq\_ref} - \omega_g \left(L_q \cdot i_{gq} - \Psi_{sm}\right) \end{cases} \tag{21}$$

The expressions in Equation (21) allow generating the reference voltages available at the output of the PI controllers of the direct and quadrature current regulation loops.

The PI controllers are synthesized using the pole placement technique for the closed-loop dynamics. The open-loop transfer function is presented in Equation (22) [29].

$$FTBO = \frac{K_i}{s}\left(1 + \frac{K_p}{K_i} s\right)\left(\frac{\dfrac{1}{R_{gss}}}{1 + \dfrac{L_d}{R_{gss}}}\right) \tag{22}$$

Using the pole compensation method, we obtain Equation (23) which gives the time constant of the original system.

$$\tau_{co} = \frac{L_d}{R_{gss}} = \frac{K_p}{K_i} \tag{23}$$

The open-loop transfer function thus reduces to (24).

$$FTBO = \frac{K_i}{s \cdot R_{gss}} \tag{24}$$

In closed loop, the expressions in Equation (25) are used, with τ_{cf} being the time constant of the reduced closed-loop system.

$$\begin{cases} FTBF = \dfrac{1}{s \cdot \tau_{cf} + 1} \\ \tau_{cf} = \dfrac{R_{gss}}{K_i} \end{cases} \tag{25}$$

A response time τ_{rc} of the closed-loop system to reach 95% of the setpoint allows calculating the controller parameters, as indicated by the expressions in (26).

$$\begin{cases} K_i = \dfrac{3R_{gss}}{\tau_{rc}} \\ K_p = \dfrac{3L_d}{\tau_{rc}} \end{cases} \tag{26}$$

3. Results and Discussion

Three cases are simulated. In the first case, we set $\beta = 1^\circ$ with $C_{p\max} = 0.4234$ and $\lambda_{op} = 7.552$ for a nominal and ideal wind speed of 11.5 m/s. In the second case, the pitch angle is regulated by the controller we proposed. The third case considers three realistic wind speeds of 9 m/s, 11.5 m/s, and 22 m/s applied to the turbine at regular time intervals of 100 s. We focused on the evolution of the turbine rotational speed, the electromagnetic torque and power, the Id and Iq currents, and the AC voltages and currents.

3.1. Simulation Case 1

The curves in **Figure 3** show the evolution of the rotational speed, electromagnetic torque, and electromagnetic power for a nominal wind speed of 11.5 m/s.

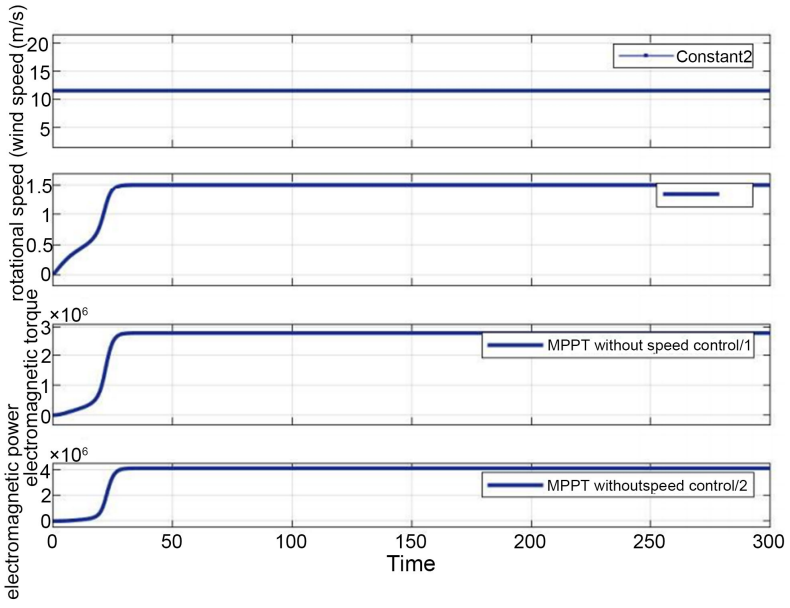

Figure 3. Evolution of the dynamic parameters with $\beta = 1^\circ$ for ideal wind.

It can be observed that the nominal values of the turbine speed and power are exceeded, reaching 1.5 rad/s for speed and over 4 MW for power. This phenomenon can be controlled by a pitch angle controller.

3.2. Simulation Case 2

The curves in Figure 4 show the evolution of the rotational speed, electromagnetic torque, and electromagnetic power for an ideal nominal wind speed of 11.5 m/s in the presence of the pitch controller.

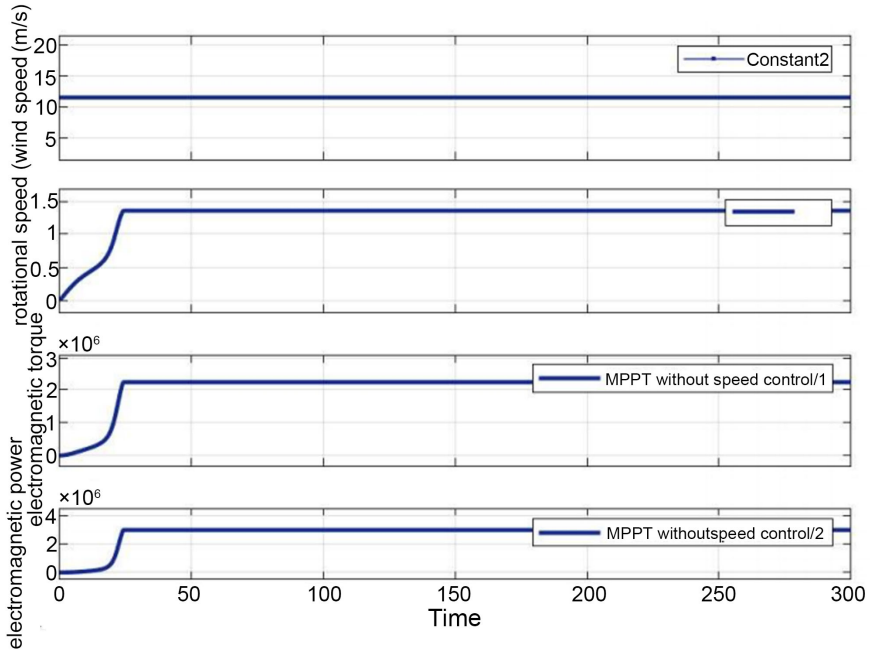

Figure 4. Evolution of the dynamic parameters with pitch control for ideal wind.

In Figure 4, It can be observed that the nominal values of the turbine speed and power are kept within their limits: 1.348 rad/s for speed and 3 MW for power. The pitch controller thus not only optimizes the extracted power but also maintains the power at its nominal value. By keeping $\beta = 1^{\circ}$ for low and medium wind speeds, the power coefficient can be adjusted to achieve an aerodynamic power of 3 MW at 11.5 m/s. However, this approach does not allow optimizing the electrical power, which increases with aerodynamic efficiency at low values of β. This aspect is managed by the pitch angle controller. Nevertheless, it is necessary to evaluate the controller's performance in limiting the power under strong and realistic wind dynamics.

3.3. Simulation Case 3

The curves in Figure 5 show the evolution of the rotational speed, electromagnetic torque, and electromagnetic power for three realistic wind speeds—9 m/s, 11.5 m/s, and 22 m/s—in the presence of the pitch controller over a period of 300 s.

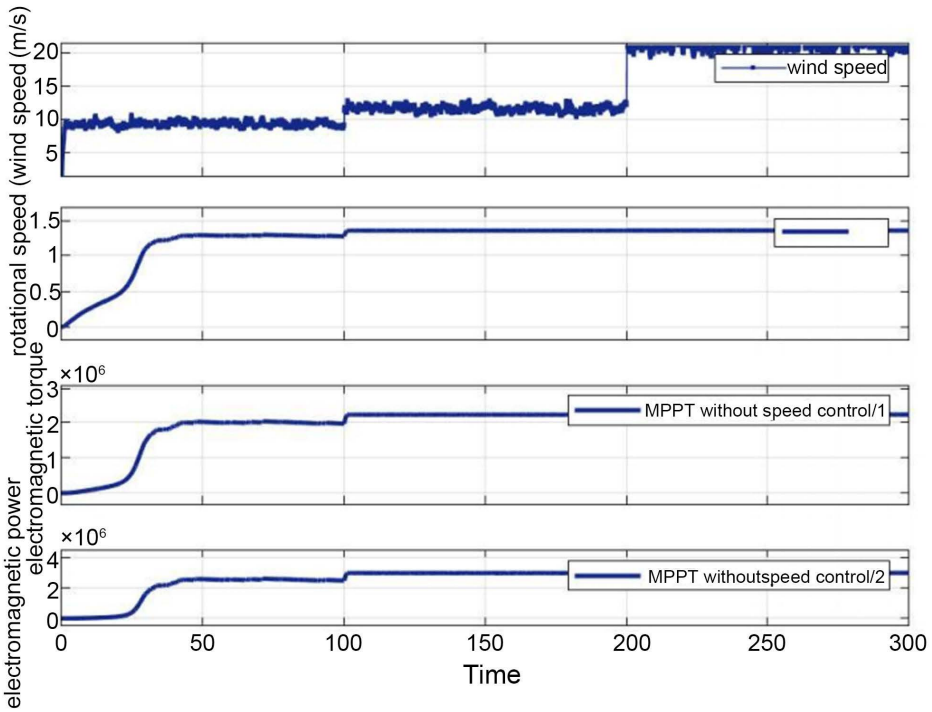

Figure 5. Evolution of the dynamic parameters with pitch control for realistic wind.

In Figure 5, it can be observed that the nominal values of the turbine speed and power are maintained within their limits: 1.348 rad/s for speed and 3 MW for power. The pitch controller thus optimizes and limits the extracted power over a wide range of wind speeds, demonstrating the robustness of the pitch controller. This performance is achieved with a proportional gain of 26.765. However, the high gain value may alter the gain margin of the timing angle. This can be corrected by introducing a primary system or by using programmed gain correctors.

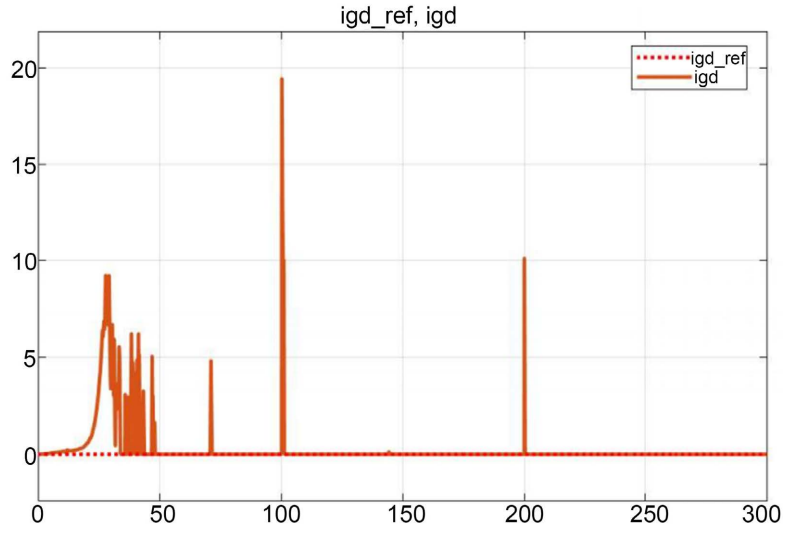

Figure 6. Evolution of the Id current and its reference in the PMSG.

Figure 6 shows that the Id current in the GSAP closely follows its zero-reference value, with peaks appearing at moments of sudden wind speed changes.

In Figure 7, the Iq current also follows its reference, displaying a pattern similar to the rotational speed. Indeed, the Iq current is proportional to the square of the speed due to the MPPT algorithm of the electromagnetic torque applied to the turbine. The Id and Iq currents evolving near their references demonstrate that the decoupling is well achieved, thus ensuring proper operation of the vector control.

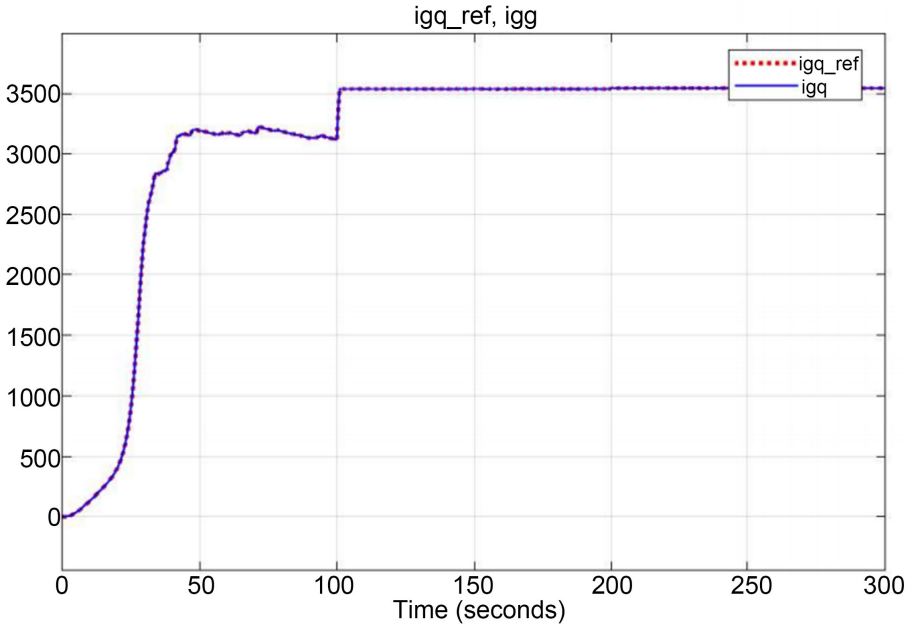

Figure 7. Evolution of the Iq current and its reference in the PMSG.

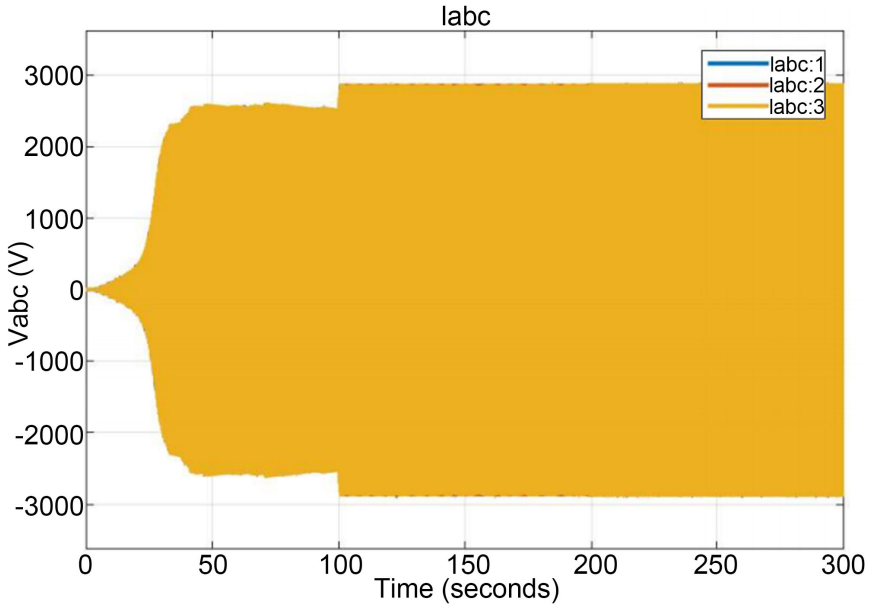

Figure 8. Evolution of the three-phase currents Iabc in the PMSG.

Figure 8 and Figure 9 respectively show that the three-phase generator currents and the three-phase voltages follow the speed variations under low wind conditions. However, when the wind speed exceeds the nominal value, the pitch control comes into action and limits the electrical power to its nominal value. Consequently, the GSAP currents and voltages at variable frequency, decoupled from the grid, are limited to their maximum values.

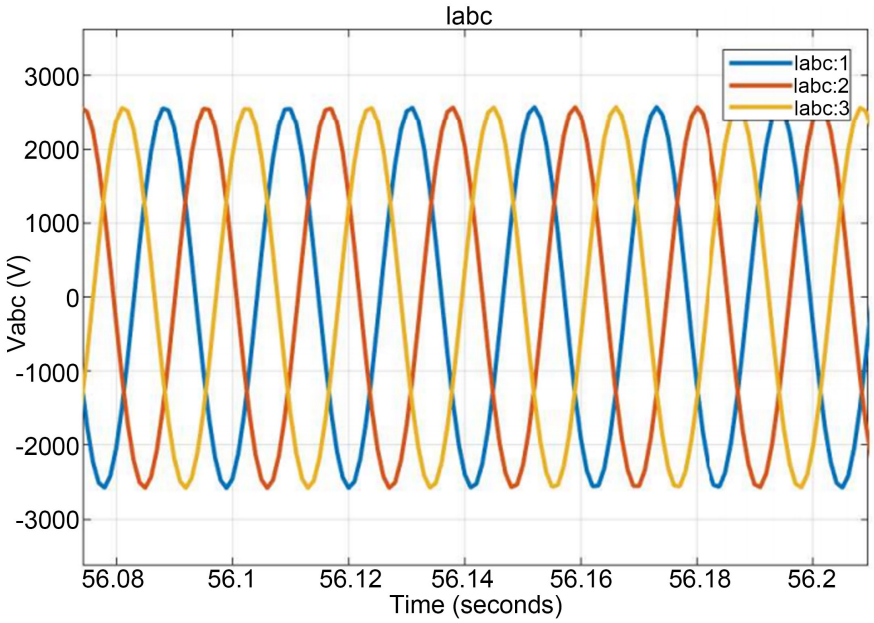

Figure 9. Zoom on the three-phase currents Iabc in the PMSG.

Figure 10 and Figure 11, which zoom in on the phase currents and phase voltages, illustrate that these quantities are sinusoidal.

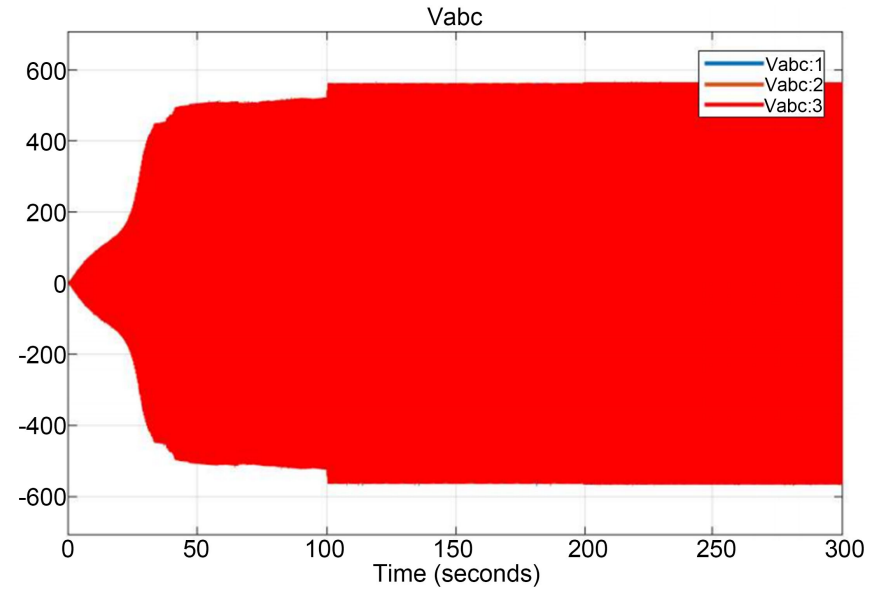

Figure 10. Evolution of the three-phase voltages Vabc at the PMSG output.

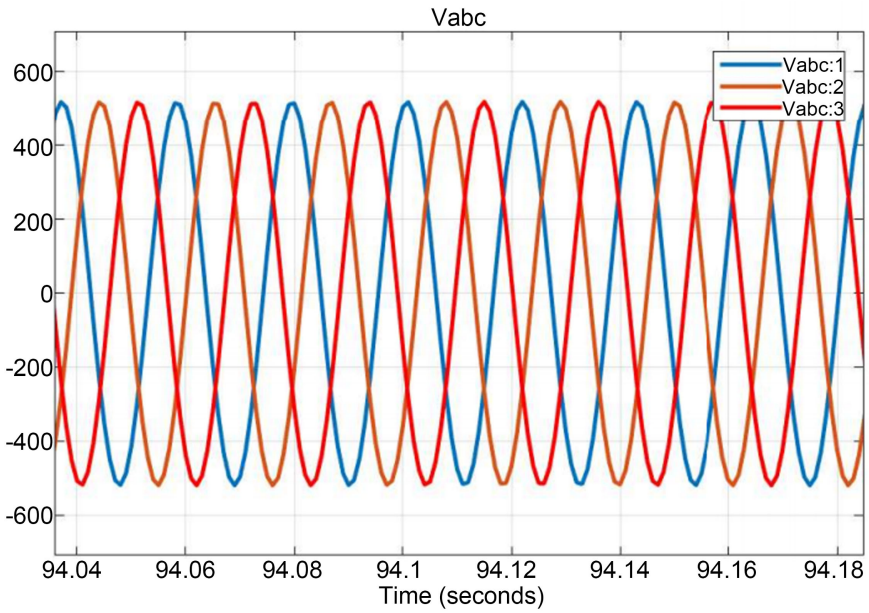

Figure 11. Zoom on the three-phase currents Vabc in the PMSG.

4. Conclusions

In the context of promoting wind energy development in Benin, we modeled the components of the energy conversion chain of a variable-speed wind turbine of the E115/3M type in order to evaluate its behavior under fluctuating wind conditions. The electrical converter is a high-pole permanent magnet generator. The control of the electromagnetic torque using an MPPT algorithm without speed regulation allowed extracting the maximum electrical power at low wind speeds. For realistic medium and high wind speeds, the action of the blade pitch regulation system, based on a proportional controller with memory, limited the power to 3 MW. The ability of the pitch controller to maintain the power at its nominal value despite wind speed fluctuations demonstrates its robustness, speed, and precision, ensuring stable and safe operation of the wind turbine. The pitch controller not only efficiently limits the power at full load and optimizes power at partial load, but it also has the advantage of being simple and less computationally demanding. Its simplicity facilitates integration into an optimization algorithm, particularly for stability studies.

However, the high gain value may alter the gain margin of the pitch angle. This can be corrected by introducing a first-order system or by using controllers with scheduled gains.

The synchronous generator is modeled in the two-phase reference frame. Vector control is used to decouple the voltages and align the flux along the quadrature axis. Validation tests showed that the Id and Iq currents evolve near their reference values, demonstrating that the decoupling is properly achieved and thus ensuring the correct operation of the vector control and the entire system.

Power optimization and safe operation at nominal power facilitate the integration of wind energy into the electricity mix of countries like Benin.

Conflicts of Interest

The authors declare no conflicts of interest regarding the publication of this paper.

References

[1] El Yaakoubi, A. (2018) Wind Energy Conversion Systems Control for Maximum Power Capture and Excessive Loads Alleviation. Ph.D. Thesis, Abdelmalek Essaadi University.

[2] EL Yaakoubi, A. and Amhaimar, L. (2022) Contrôle optimal de l'angle de calage des pales pour limiter la puissance produite et réduire les charges mécaniques des aéro turbines. *UPB Scientific Bulletin*, *Series D*, **84**, 235-250.

[3] (2018) Plan directeur de la cedeao pour le développement des moyens régionaux de production et de transport d'energie electrique 2019-2033. TOME 1: Résumé Exécutif. https://www.ecowapp.org/sites/default/files/tome_1.pdf

[4] Ayadi, B. (2020) Élaboration du code réseau (ht/mt) de la société béninoise d'energie électrique. https://are.bj/storagebjarehightsecurity/2021/05/Code_Reseau_SBEE_HT-MT.pdf

[5] (2003) Décret du 27 juin 2003 "Prescriptions techniques générales de conception et de fonctionnement auxquelles doivent satisfaire les installations en vue de leur raccordement au réseau public de transport de l'électricité". Ministère de l'économie, des finances et de l'industrie.

[6] Jiao, X., Yang, Q. and Xu, B. (2021) Hybrid Intelligent Feedforward-Feedback Pitch Control for VSWT with Predicted Wind Speed. *IEEE Transactions on Energy Conversion*, **36**, 2770-2781. https://doi.org/10.1109/tec.2021.3076839

[7] Ribrant, J. and Bertling, L.M. (2007) Survey of Failures in Wind Power Systems with Focus on Swedish Wind Power Plants during 1997-2005. *IEEE Transactions on Energy Conversion*, **22**, 167-173. https://doi.org/10.1109/tec.2006.889614

[8] Salles, M.B.C., Hameyer, K., Cardoso, J.R. and Freitas, W. (2008) Dynamic Analysis of Wind Turbines Considering New Grid Code Requirements. 2008 18*th International Conference on Electrical Machines*, Vilamoura, 6-9 September 2008, 1-6. https://doi.org/10.1109/icelmach.2008.4799899

[9] Chondrogiannis, S. and Barnes, M. (2008) Stability of Doubly-Fed Induction Generator under Stator Voltage Orientated Vector Control. *IET Renewable Power Generation*, **2**, 170-180. https://doi.org/10.1049/iet-rpg:20070086

[10] Deng, X., Yang, J., Sun, Y., Song, D., Yang, Y. and Joo, Y.H. (2020) An Effective Wind Speed Estimation Based Extended Optimal Torque Control for Maximum Wind Energy Capture. *IEEE Access*, **8**, 65959-65969. https://doi.org/10.1109/access.2020.2984654

[11] Yin, M., Li, W., Chung, C.Y., Zhou, L., Chen, Z. and Zou, Y. (2017) Optimal Torque Control Based on Effective Tracking Range for Maximum Power Point Tracking of Wind Turbines under Varying Wind Conditions. *IET Renewable Power Generation*, **11**, 501-510. https://doi.org/10.1049/iet-rpg.2016.0635

[12] Abdullah, M.A., Yatim, A.H.M., Tan, C.W. and Saidur, R. (2012) A Review of Maximum Power Point Tracking Algorithms for Wind Energy Systems. *Renewable and Sustainable Energy Reviews*, **16**, 3220-3227. https://doi.org/10.1016/j.rser.2012.02.016

[13] Muljadi, E. and Butterfield, C.P. (2001) Pitch-Controlled Variable-Speed Wind Turbine Generation. *IEEE Transactions on Industry Applications*, **37**, 240-246.

https://doi.org/10.1109/28.903156

[14] Bonfiglio, A., Delfino, F., Gonzalez-Longatt, F. and Procopio, R. (2017) Steady-State Assessments of PMSGs in Wind Generating Units. *International Journal of Electrical Power & Energy Systems*, **90**, 87-93. https://doi.org/10.1016/j.ijepes.2017.02.002

[15] Boldea, I. (2016) Synchronous Generators. Second Edition, Taylor and Francis Group, 125-145.

[16] Ezzat, M. (2011) Commande Non Linéaire Sans Capteur de La Machine Synchrone à Aimants Pennanents. Master's Thesis, École Centrale de Nantes.

[17] ENERCON (2013) Description technique SCADA Système ENERCON. https://www.haute-saone.gouv.fr/index.php/contenu/telechargement/13454/108561/file/Etude+de+dangers-annexes.pdf

[18] ENERCON GmbH, Dreekamp 5, D-26605 Aurich, Allemagne. https://fr.kompass.com/c/enercon-gmbh/de642099/

[19] Milano, F. (210) Power System Modelling and Scripting (Power Systems). Springer.

[20] Le Gourières, D. (1982) Energie éolienne. Théorie, conception et calcul pratique des installations, deuxième edition. Eyrolles.

[21] Chakraborty, S., Kramer, B. and Kroposki, B. (2009) A Review of Power Electronics Interfaces for Distributed Energy Systems Towards Achieving Low-Cost Modular Design. *Renewable and Sustainable Energy Reviews*, **13**, 2323-2335. https://doi.org/10.1016/j.rser.2009.05.005

[22] Mena Lopez, H.E. (2007) Maximum Power Tracking Control Scheme for Wind Generator Systems. Ph.D. Thesis, Texas A&M University.

[23] Robyns, B., Davigny, A., François, B., Henneton, A. and Sprooten, J. (2012) Electricity Production from Renewable Energies. ISTE Ltd., 45-146.

[24] Hanzo, L. (2011) Power Conversion and Control of Wind Energy Systems. Edition IEEE Press.

[25] Elbeji, O., Hamed, M.B. and Sbita, L. (2014) PMSG Wind Energy Conversion System: Modeling and Control. *International Journal of Modern Nonlinear Theory and Application*, **3**, 88-97. https://doi.org/10.4236/ijmnta.2014.33011

[26] Louar, F. (2016) Modélisation et simulation d'une chaine de conversion d'énergie éolienne à base d'une machine synchrone à aimant permanent. Master's Thesis, Université Bdji Mokhtar de Annaba.

[27] Meghni, B. (2015) Contribution à l'amélioration des performances d'une chaine énergétique eolienne. Master's Thesis, Université Bdji Mokhtar de Annaba.

[28] Babaie Lajimi, A., Asghar Gholamian, S. and Shahabi, M. (2011) Modeling and Control of a DFIG-Based Wind Turbine during a Grid Voltage Drop. *Engineering, Technology & Applied Science Research*, **1**, 121-125. https://doi.org/10.48084/etasr.60

[29] Aimani, E. (2004) Modélisation de différentes technologies d'éoliennes intégrées dans un réseau de moyenne tension. Master's Thesis, Ecole centrale de Lille. http://l2ep.univ-lille1.fr/fileupload/file/theses/SalmaElAimani.pdf